

Ocean eddy momentum fluxes at the latitudes of the Gulf Stream and the Kuroshio extensions as revealed by satellite data

Richard John Greatbatch · Xiaoming Zhai ·
Jan-Dirk Kohlmann · Lars Czeschel

Received: 1 December 2009 / Accepted: 24 February 2010 / Published online: 25 March 2010
© Springer-Verlag 2010

Abstract Eddy momentum fluxes, i.e. Reynold stresses, are computed for the latitude bands of the Gulf Stream and Kuroshio extensions using 13 years of data from the merged satellite altimeter product of Le Traon et al. The spatial pattern and amplitude of the fluxes is remarkably similar to that found by Ducet and Le Traon using the 5 years of data that were available to them. In addition to updating the work of Ducet and Le Traon, we provide new insight into the role played by the underlying variable bottom topography, both for determining the structure of the eddy momentum fluxes seen in the satellite data and for influencing the way these fluxes feedback on the mean flow. While there is no clear evidence that eddies locally flux momentum into the eastward jets of the Gulf Stream and Kuroshio extensions, a clearer picture emerges after zonally integrating across each of the North Atlantic and North Pacific basins. We argue that the eddy momentum fluxes do indeed drive significant transport, a conclusion supported by preliminary results from a 3-D model calculation. We also present evidence that in the North Pacific, the Reynolds stresses are important for driving the recirculation gyres associated with the Kuroshio extension, taking advantage of new data from both observations and high-resolution model simulations.

Keywords Reynolds stresses · Ocean momentum fluxes · Recirculation gyres

1 Introduction

In the atmosphere, fluxes of momentum by the synoptic eddies are known to play a fundamental role in the dynamics of both the mean circulation (e.g. Holton 1981; Vallis 2006; Marshall and Plumb 2008) and the low frequency variability, notably in the dynamics of the annular modes and, in particular, the North Atlantic Oscillation (e.g. Limpasuvan and Hartmann 1999; Greatbatch 2000; Thompson et al. 2002; Benedict et al. 2004; Kunz et al. 2009). Distortion of the eddy shape from exact circular symmetry can lead to a positive feedback between the background flow and the eddy momentum fluxes (e.g. Shutts 1983; Hoskins et al. 1983; Haines and Marshall 1987). A well-known example is that of banana-shaped eddies commonly observed in association with the mid-latitude westerly jet stream (see Figure 8.14 in Marshall and Plumb 2008 and the discussion thereon) for which there is a positive feedback between the advective distortion of the eddies by the jet and the resulting eddy flux of westerly momentum into the jet (see also Wardle and Marshall 2000). Thompson (1971) had previously noted that Rossby wave radiation out of a westerly jet, such as the Gulf Stream, is associated with a flux of westerly momentum into the jet, a mechanism he put forward to explain the sharpness of the westerly jet stream in the atmosphere and eastward currents in the ocean such as the Gulf Stream and Kuroshio extension. Even earlier than Thompson, Webster (1965) had presented evidence of an eddy flux of momentum in the Florida Current towards regions of high flow speed, implying a “negative eddy viscosity”. More

Responsible Editor: Dirk Olbers

R. J. Greatbatch (✉) · J.-D. Kohlmann · L. Czeschel
Leibniz-Institut für Meereswissenschaften, IFM-GEOMAR,
Kiel, Germany
e-mail: rgreatbatch@ifm-geomar.de

X. Zhai
Atmospheric, Oceanic and Planetary Physics,
University of Oxford,
Oxford, UK

recently, comparing two numerical model experiments, differing only in that one contains mesoscale eddies and the other does not, Zhai et al. (2004) find stronger Gulf Stream recirculation gyres in the Gulf Stream extension region in the experiment with eddies than in the experiment without eddies. However, Zhai et al. do not explicitly show that the difference is because of the eddy momentum fluxes in the experiment with eddies.

Nevertheless, the situation in the ocean is more complex than that in the atmosphere. There are some in situ measurements, though sparse, in support of the claim that eddies flux momentum upgradient in order to help maintain currents such as the Gulf Stream and Kuroshio, e.g. Webster (1965), Schmitz (1982), Nishida and White (1982). Satellite observations, on the other hand, provide a unique opportunity to study the mesoscale variability in the ocean with a high spatial and temporal resolution, as well as global coverage, and some work has been done to study the influence of mesoscale eddies on the large-scale mean flow (e.g. Tai and White 1990; Kelly 1991; Morrow et al. 1992; Qiu 1995; Adamec 1998; Stammer and Wunsch 1999; Ducet and Le Traon 2001; Hughes and Ash 2001). However, the picture that emerges from these studies is complex, e.g. eddies can act to accelerate the mean flow in some regions and decelerate it in others. There also appear to be multiple jets that are related to features of the bottom topography (Hughes and Ash 2001). Ducet and Le Traon (2001), who used 5 years of merged TOPEX/Poseidon and ERS-1/2 altimetric data to study eddy kinetic energy (EKE) and Reynolds stresses in the Gulf Stream and Kuroshio region, noted the complex patterns seen in the Reynolds stresses and attributed features in both the EKE and Reynolds stress fields to the underlying bottom topography. Indeed, in contrast to the atmosphere (especially over the oceanic regions of the atmospheric storm tracks), eddies in the ocean are subject to influence from rough and steep bottom topography that has considerable spatial variability. It seems likely that it is the distortion of the eddies by the variable bottom topography that leads to the much more complex relationship between the mean flow and the eddies in the ocean. An early example of this behaviour is provided by Böning (1989) who noted that including rough bottom topography in an eddying, ocean model with basin geometry suppressed the tendency for the flow to barotropise. Indeed, whereas in his flat-bottom model, the low frequency variability is dominated by zonally orientated bands of barotropic flow, this behaviour is completely suppressed in the same model when rough bottom topography is included.

In this paper, we re-examine the time-averaged eddy momentum fluxes for the North Atlantic and North Pacific, respectively, updating the study of Ducet and Le Traon (2001) using the longer time series of data available to us. We offer new insights into the role played by the

underlying bottom topography in both constraining the eddy momentum fluxes and in determining how these eddy fluxes modify the mean flow. Indeed, since the eddy momentum fluxes act over the whole depth of the water column, the impact of these fluxes on the mean flow must inevitably be influenced by the underlying variable bottom topography. Consistent with Ducet and Le Traon (2001), we reveal, once again, the complex nature of the eddy momentum fluxes when viewed from a local perspective. Zonally integrating across the basin leads to a more coherent picture which we interpret in terms of the recirculation gyres for both the Gulf Stream (e.g. Hogg et al. 1986) and the Kuroshio (e.g. Jayne et al. 2009). Indeed, recent observational and high-resolution modelling work has provided much new and valuable data on the recirculation gyres of the Kuroshio that aids considerably in our interpretation of the satellite-derived momentum fluxes. A feature of our results is the evidence of strong variability in the eddy fluxes on monthly time scales, even though the fluxes computed from the 13 years of data available to us are very similar to the fluxes computed using the 5 years of data available to Ducet and Le Traon (2001).

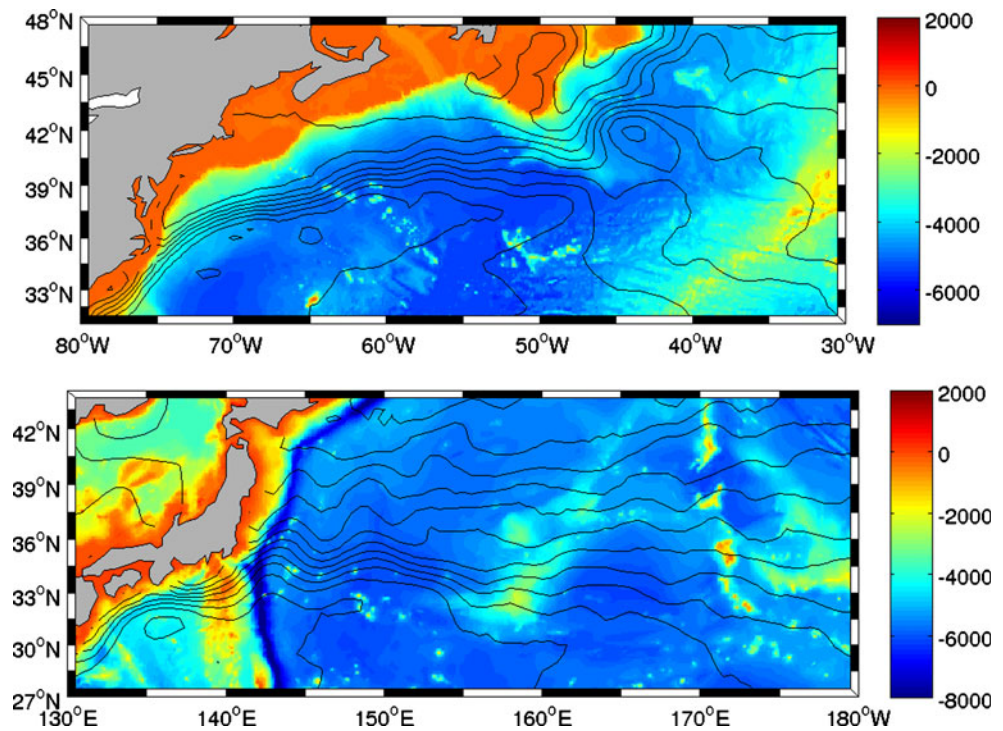
2 Data

To compute the eddy momentum fluxes, we use the surface geostrophic velocity anomaly, u' , for the period from January 1995 to December 2007 that is computed from the global sea surface height anomaly dataset compiled by the CLS Space Oceanographic Division of Toulouse, France. This dataset merges the TOPEX/POSEIDON and ERS-1/2 along-track sea surface height measurements to give temporal resolution of a week and spatial resolution of $1/3^\circ \times 1/3^\circ$ in latitude and longitude. For a detailed description of the dataset, readers are referred to Le Traon et al. (1998). The mean over the whole time series is removed from the zonal and meridional velocity anomalies before computing the fluxes. However, no attempt is made to remove the seasonal cycle (the seasonal cycle of the mean flow is, in fact, weak compared to the eddy variability and can be safely neglected).

3 Results

Figure 1 shows the bottom topography (colour shading in metres) and the mean sea surface height (contour interval 0.1 m) in the region of the Gulf Stream (top panel) and Kuroshio (lower panel) extensions. The mean sea surface height contours, taken from Niiler et al. (2003), reveal the surface geostrophic flow of the eastward jets. In the case of the Gulf Stream, the mean flow separates from the North

Fig. 1 The bottom topography (colour shading with units of metres) and the mean sea surface height (contour interval 0.1 m; from Niiler et al. 2003) in the regions of both the Gulf Stream (*upper panel*) and Kuroshio (*lower panel*) extensions



American coast at Cape Hatteras and then reconnects with the continental slope over the Southeast Newfoundland Rise (the ridge that extends southeastwards from the tail of the Grand Banks of Newfoundland near 50°W). The main part of the flow then follows the continental slope northwards to form the North Atlantic Current. The surface signature of the anticyclonic Mann Eddy (Mann 1967) can be seen in the Newfoundland Basin, just to the north of the Southeast Newfoundland Rise (see Clarke et al. 1980 for a description of the flow in this area). The New England Seamounts are also evident, extending southeastwards and crossing the path of the Gulf Stream between 65 and 60°W. It should be noted that the northern recirculation gyre sits in the region between the Gulf Stream path and the continental slope to the north, extending roughly from the Grand Banks of Newfoundland to the New England Seamounts (e.g. Hogg and Stommel 1985; Hogg et al. 1986 and Qiu 1994). In the case of the Kuroshio (lower panel), the separated jet is dominated by the large meanders immediately to the east of Japan and there is a notable tendency for the flow to diverge as it approaches the Shatsky Rise (located between 155 and 160°E) as described, for example, in Qiu et al. (2008).

Next, we note that the horizontal momentum equations appropriate to the ocean are given by

$$\frac{\partial u}{\partial t} + \mathbf{u} \cdot \nabla_h \mathbf{u} - f v = -\frac{1}{\rho_0} \frac{\partial p}{\partial x} + \frac{F_x}{\rho_0} \quad (1)$$

$$\frac{\partial v}{\partial t} + \mathbf{u} \cdot \nabla_h \mathbf{v} + f u = -\frac{1}{\rho_0} \frac{\partial p}{\partial y} + \frac{F_y}{\rho_0} \quad (2)$$

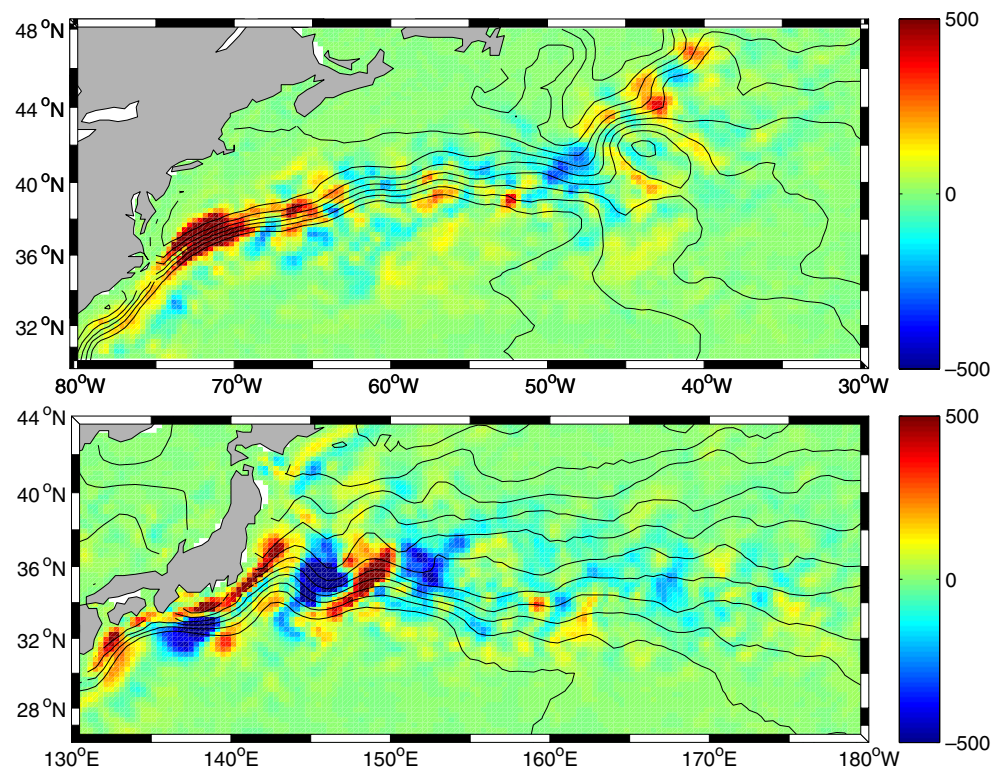
where, the advection term is written using the horizontal gradient operator, p is pressure, \mathbf{u} is the horizontal velocity (u and v are its zonal and meridional components, respectively), and (F_x, F_y) is the frictional force, including the wind forcing. (Note that the vertical advection of momentum, which is not of interest here, has been neglected. It should be noted that this term is small compared to the horizontal advection terms when the flow is close to being in geostrophic balance.) Taking a long time average gives

$$\frac{\partial \bar{u}}{\partial t} + \bar{u} \frac{\partial \bar{u}}{\partial x} + \bar{v} \frac{\partial \bar{u}}{\partial y} - f \bar{v} = -\frac{\partial \overline{u'u'}}{\partial x} - \frac{\partial \overline{u'v'}}{\partial y} - \frac{1}{\rho_0} \frac{\partial \bar{p}}{\partial x} + \frac{\bar{F}_x}{\rho_0} \quad (3)$$

$$\frac{\partial \bar{v}}{\partial t} + \bar{u} \frac{\partial \bar{v}}{\partial x} + v \frac{\partial \bar{v}}{\partial y} + f \bar{u} = -\frac{\partial \overline{v'v'}}{\partial x} - \frac{\partial \overline{v'u'}}{\partial y} - \frac{1}{\rho_0} \frac{\partial \bar{p}}{\partial y} + \frac{\bar{F}_y}{\rho_0} \quad (4)$$

Figure 2 shows plan views of the 13-year average of the Reynolds stress co-variance $u'v'$ for the regions of both the Gulf Stream and Kuroshio extensions together with the mean sea surface height contours to indicate the mean flow by geostrophy. For comparison, Fig. 3 reproduces Plate 8 from Ducet and Le Traon (2001). It should be noted that we have used 13 years of data compared to the 5 years available to Ducet and Le Traon (2001). Interestingly, the principal features in the Reynolds stress covariance are clearly the same in both figures, even if there are some differences in detail. In the case of the Kuroshio, the alternating positive and negative bands between Japan and

Fig. 2 The 12-year average of the Reynolds stress cross-covariance $u'v'$ for the Gulf Stream (*upper panel*) and the Kuroshio (*lower panel*). Units are cm^2s^{-2} . The *solid lines* show the mean sea surface height contours taken from Niiler et al. (2003) plotted at 10-cm intervals



150°E (clearly related to the meanders of the mean flow), the negative band between 150 and 160°E and even the positive values near 160°E, are common to both Figs. 2 and 3. Likewise, in the case of the Gulf Stream, there are many common features; for example the “double blade” structure immediately following the separation of the mean flow from the coast near Cape Hatteras that was noted by Ducet and Le Traon (2001), the impact of the New England Seamounts to the southeast of Cape Cod, the tendency for negative values south of Atlantic Canada, and the two lines of positive values on either side of the Mann Eddy and associated with the Southeast Newfoundland Rise to the southwest and the Newfoundland Seamounts to the north. The constancy of these features, despite the longer averaging period we have used, is indicative of their robustness and is consistent with the idea that bottom topography plays an important role in locking these features in place. On the other hand, it is difficult to see consistent evidence of positive values being found to the south of the two currents and negative values to the north, as one would expect if the eddies were fluxing westerly momentum into the two jets. The impression is rather of alternating bands of positive and negative values following the mean flow. Figures 4 and 5 shows plots of the 13-year average of $u'u'$ and $v'v'$, respectively, for the same regions. Again, the principal features can be found in the corresponding plots shown in Ducet and Le Traon (2001) (their Plates 1 and 2 not repeated here). As noted by Ducet and Le Traon (2001), the terms

involving $u'u'$ and $v'v'$ in Eq. 3 and Eq. 4 are not small compared to the term involving $u'v'$ (see Plate 9 in Ducet and Le Traon 2001) and cannot be neglected when considering the local momentum balance. Nevertheless, the initial impression is that it is difficult to see any coherent eddy forcing of the mean flow that is associated locally with the Reynolds stresses.

Returning to Fig. 2, the two most prominent features of the Reynolds stress co-variance $u'v'$ in the Gulf Stream region are the double-blade feature associated with positive fluxes (red) near the separation point and the region of negative fluxes (blue) near the tail, and slightly to the west of, the Grand Banks of Newfoundland. Although not immediately evident from the figure, the feature near Cape Hatteras reaches an amplitude of near $1,500 \text{ cm}^2\text{s}^{-2}$ compared to about $500 \text{ cm}^2\text{s}^{-2}$ in the case of the feature near the Grand Banks. It is worth pointing out that both of these features can be explained by flow variations along the direction of the mean flow, indicating that the variability has a preference for such variability. At both locations, the flow is constrained by the neighbouring continental slope (see Fig. 1) which near Cape Hatteras encourages flow in the southwest/northeast direction, as exhibited by the mean flow, and near the Grand Banks in the northwest/southeast direction. The tendency for the flow variability to be orientated in these directions at these locations is also evident from the angle of the major axis of the covariance ellipse plotted in Fig. 5 of Scott et al. (2009; this is especially clear near Cape

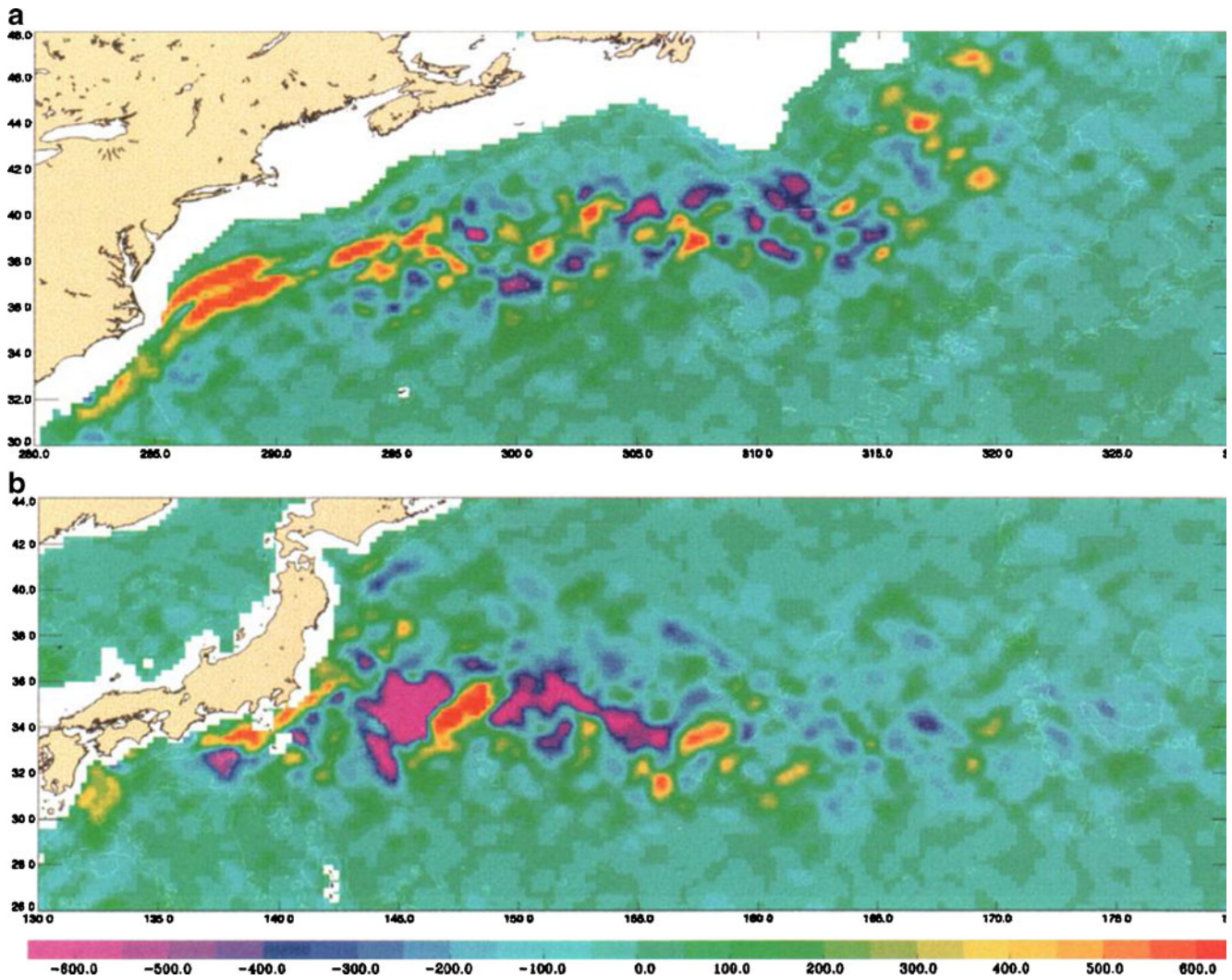
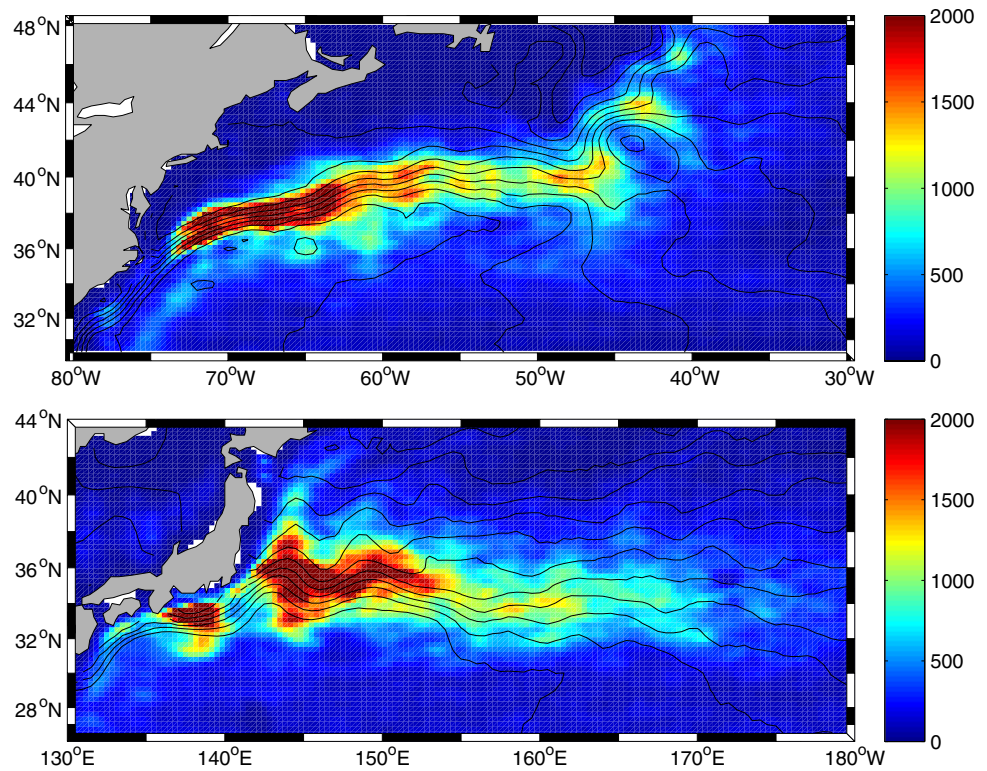


Fig. 3 As Fig. 2 but from Ducet and Le Traon (2001) and based on 5 years of data

Hatteras, rather less clear near the Grand Banks). We shall argue later (in Section 4) that these features play a role in driving the northern recirculation gyre of the Gulf Stream; indeed they are the major features to emerge in the analysis of the zonally integrated momentum budget described below. In the case of the Kuroshio, the region of negative fluxes just south of Japan and near 137°E is related to the appearance of the Kuroshio Large Meander (Taft 1972; Kawabe 1985). Note, in particular, that when the meander is present, the region of negative fluxes (blue) is associated with anomalous flow that is both southward and eastward on the west side of the meander, with the smaller region of positive fluxes (red) immediately to the east being associated with the anomalous northward and eastward flow on its east side. As in the case of the Gulf Stream near Cape Hatteras, there is a band of positive (red) fluxes near the coast of Japan that almost certainly results from the topographic blocking of the flow

there by the steep continental slope (see Fig. 1) and the resulting tendency for flow to vary predominantly in the southwest/northeast direction. Once the Kuroshio has separated from the coast, the Reynolds stress covariance fluxes are clearly linked to the large, quasi-stationary meanders of the mean flow. It is noticeable that the sign of the fluxes can be explained by pulsing the flow along its mean path, with positive fluxes (red) where the mean flow is both northward and eastward and negative fluxes (blue) where the mean flow is both southward and eastward. As pointed out by Qiu and Chen (2009; see also Qiu and Chen 2005), the Kuroshio Extension exhibits two basic modes of variability, a stable state in which the flow basically follows the mean state but with enhanced flow speed, and an unstable state characterised by a much higher level of eddy kinetic energy, a more southerly flow path and a reduced flow speed. The stable state clearly leads to Reynolds stress covariance fluxes like

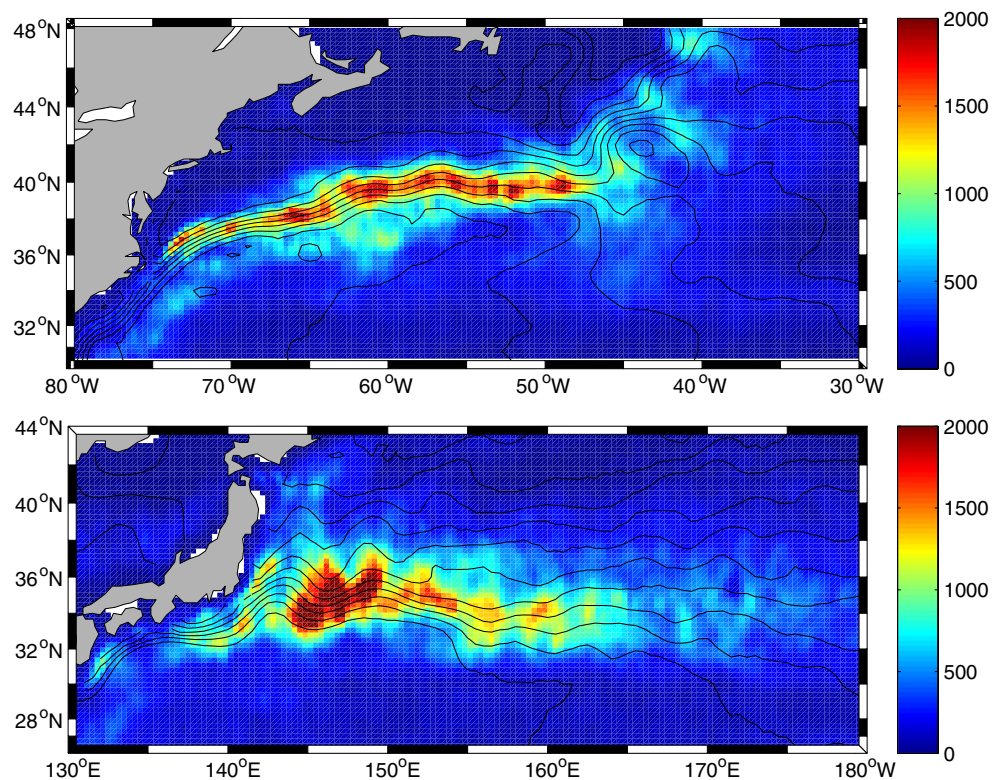
Fig. 4 The 12-year average of $u'u'$ for the Gulf Stream (*upper panel*) and Kuroshio (*lower panel*). Units are cm^2s^{-2} . The solid contours show the mean sea surface height, as in Fig. 2



those shown in Fig. 2. Qiu and Chen (2009) also note that the eddy vorticity fluxes in the Kuroshio Extension region act to maintain the quasi-stationary eddies against dissipation. However, consideration of the time-averaged

meridional momentum equation (Eq. 4 above) shows that the momentum flux convergence from the $u'v'$ term plotted in Fig. 2 acts differently from the claim in Qiu and Chen (2009), accelerating the northward flow where there is a

Fig. 5 The 12-year average of $v'v'$ for the Gulf Stream (*upper panel*) and Kuroshio (*lower panel*). Units are cm^2s^{-2} . The solid contours show the mean sea surface height, as in Fig. 2



ridge and decelerating the northward flow where there is a trough.

To try and make some sense of the Reynolds stresses, we now consider their contribution to the zonally integrated momentum budget for the zonal flow. Zonally integrating Eq. 3 gives

$$\frac{\partial}{\partial t} \langle \bar{u} \rangle + \frac{\partial}{\partial y} \langle \bar{v}\bar{u} \rangle - f \langle \bar{v} \rangle = - \frac{\partial \langle \overline{u'v'} \rangle}{\partial y} + \langle \frac{\bar{F}_x}{\rho_0} \rangle \tag{5}$$

where an overbar continues to mean time average, deviations from the time average are denoted by a prime and $\langle \rangle$ denotes a zonal integral across the basin. The eddy momentum forcing of the zonally integrated zonal flow depends on the convergence of the meridional eddy flux of zonal momentum (the first term on the right hand side of Eq. 5). Indeed, a feature of the zonally integrated balance Eq. 5, compared to the local balance Eq. 3, is the disappearance of the term involving $u'u'$, simplifying the interpretation. The solid blue line in Figs. 6 and 7 shows the 13 year average of $\langle u'v' \rangle$ for both the Gulf Stream and Kuroshio latitude bands plotted as a function of latitude. The outer dotted curve shows the extreme values (positive and negative) in the times series of monthly means of $\langle u'v' \rangle$ and the pink shading shows one standard deviation either side of the mean, again based on monthly means. The lower panel shows the zonal integral of the latitudinal derivative of the mean sea surface height taken from the estimate by Niiler et al. (2003). By geostrophy, this corresponds to the zonal integral of the zonal velocity.

In both cases, it is clear that while the 13- and 5-year time-averages shown in Figs. 2 and 3 are quite similar to

each other, there is considerable variability from month-to-month. Indeed, Ducet and Le Traon (2001) have already noted that there is considerable interannual variability in the momentum flux convergence associated with the Reynolds stresses (see their Plates 11 and 12). However, as can be seen from Figs. 6 and 7, the variability is confined to the latitude band occupied by the strong eastward mean flow. In the case of the Gulf Stream, the negative gradient of $u'v'$ in the latitude band of the strongest zonal mean flow between 37 and 41°N indicates that after zonally integrating, the eddy fluxes do systematically feed momentum into the jet. The maximum/minimum in the northward flux of eastward momentum near 37°N/41°N are associated with the “double blade” feature near the separation point (red in Fig. 2) and the region of southward fluxes (in blue) near the tail of the Grand Banks of Newfoundland. In the case of the Kuroshio, the picture is less clear. It appears that after zonally integrating, the eddy fluxes feed/extract westerly momentum into/out of alternating latitude bands, although there is no evidence of these bands in the zonally integrated mean flow shown in the lower panel. As we discuss in Section 4, this interpretation is misleading, partly because the mean zonal flow plotted in the lower panel is only for the surface, and does not reflect the subsurface flow, and partly because the Kuroshio has a strong zonal component as it flows along the coast of Japan prior to separation, and this zonal component contributes to the zonal integral shown in the plot.

We can ask how large is the forcing from the eddy momentum flux (the first term on the right hand side of Eq. 5) compared to the forcing from the zonally integrated

Fig. 6 Upper panel: the 12-year average $u'v'$, zonally integrated across North Atlantic and plotted as a function of latitude (solid blue line); the range of values taken by monthly averages of the zonal integral of $u'v'$ during the 12-year period (solid pink curves); and ± 1 standard deviation of monthly averages of the zonal integral $u'v'$ (pink shading). Lower panel: the zonal integral across the North Atlantic of the latitudinal derivative of the mean sea surface height taken from Niiler et al. (2003)

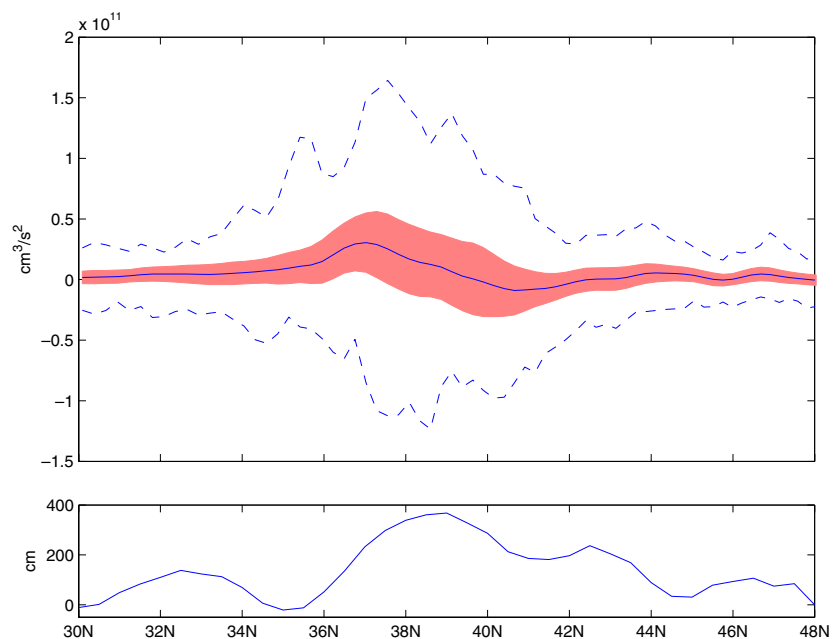
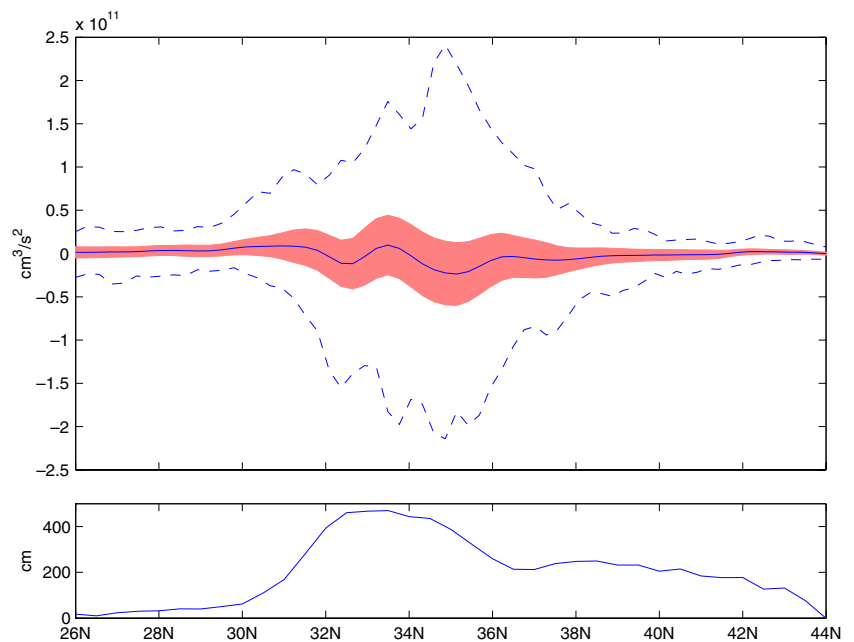


Fig. 7 Upper panel: the 12-year average $u'v'$, zonally integrated across North Pacific and plotted as a function of latitude (*solid blue line*); the range of values taken by monthly averages of the zonal integral of $u'v'$ during the 12-year period (*solid pink curves*); and ± 1 standard deviation of monthly averages of the zonal integral $u'v'$ (*pink shading*). Lower panel: the zonal integral across the North Pacific of the latitudinal derivative of the mean sea surface height taken from Niiler et al. (2003)



surface wind stress (contained in the term F_x in Eq. 5). We begin with the Gulf Stream region where the zonally integrated eddy momentum flux is feeding into the mean jet. Over the top 100 m of the water column, corresponding to the surface Ekman layer, it is easy to show that the surface wind stress dominates. However, when integrated over the depth of the ocean, and assuming the Reynolds stress decays roughly linearly from the surface to the bottom (since the eddies extend to the bottom of the ocean) the two terms become comparable in magnitude. To obtain this result, we use the gradient of the solid blue line in Fig. 6 to estimate the eddy forcing, we note that the zonally averaged zonal wind stress has magnitude roughly 0.1 Nm^{-2} , that the width of the North Atlantic is roughly 50° in longitude, and take the depth of the ocean to be 4,000 m. A similar conclusion can be reached in the case of the Kuroshio.

4 Relationship to the Gulf Stream and Kuroshio recirculation gyres

Let us now try and understand more clearly the eddy momentum fluxes and their relationship to the recirculation gyres associated with the Gulf Stream and Kuroshio extensions. In the case of the Gulf Stream extension, we have already noted that after zonally integrating, the eddies do indeed flux momentum into the zonal jet. This certainly supports the idea that the momentum forcing from the Reynolds stresses plays a role in driving the recirculation gyres of the Gulf Stream. We also noted that the two features of the momentum flux plotted in Fig. 2 that are

important in the zonally integrated zonal momentum balance are the double-blade feature (in red) near Cape Hatteras, associated with a northward flux of zonal momentum, and the southward flux of zonal momentum (in blue) near and slightly to the west of the Grand Banks of Newfoundland (around 41°N , 48°W). The latitude bands occupied by these features do indeed correspond to the latitude bands occupied by the southern and northern recirculation gyres, respectively (e.g. Worthington 1986; Schmitz 1980; Richardson 1985; Hogg et al. 1986 and Greatbatch 1987). However, as noted by Ducet and Le Traon (2001), locally the term involving $u'u'$ in Eq. 3 is also important in the local momentum balance and cannot be neglected, even though this term drops out after zonal integrating. Despite this caveat, it is of interest to consider the impact of the $u'v'$ term in Eq. 3 and, in particular, the impact of northward flux of zonal momentum near Cape Hatteras and the southward flux of zonal momentum near the Grand Banks. These two regions sit at the far eastern and western ends of the northern recirculation (see Fig. 2 and the discussion thereon, and also Fig. 6a in Qiu 1994). Furthermore, both regions are connected by f/H contours along the continental slope. Since we know that the impact of the Reynolds stresses are felt throughout the whole depth of the water column, we can consider the impact of the $u'v'$ term in the context of a barotropic, uniform density ocean linearised about a state of rest. Considering first the patch of southward momentum flux near the Grand Banks, it follows from Eq. 3 that the effect is to apply a westward acceleration on the northern side and an eastward acceleration on the southern side of the patch. These accelerations in turn will drive westward/eastward flow along the f/H

contours that cut through the northern/southern side of the patch. These flows will extend southward along the continental slope because of topographic wave propagation until they encounter the opposite forced region near Cape Hatteras where the two flows can connect to form a closed loop. In this way, a flow analogous to the northern recirculation gyre can be driven. Figure 8 shows the barotropic transport stream function from such a model (uniform density/realistic bottom topography—see Fig. 9) with one sixth degree resolution in latitude and longitude and driven by both Reynolds stress forcing terms (i.e. both the $u'u'$ and $u'v'$ terms) applied to the zonal momentum equation, and assuming that the Reynolds stresses vary linearly with depth. (The model details are described in the Appendix. Note also that the effect of including the Reynolds stress forcing for the meridional equation is small and does not greatly change the figure). It is clear that the Reynolds stress terms are capable of driving considerable transport, resembling both the northern and southern recirculation gyres in the longitude band 50–60°W. Interestingly, in this region, it is the forcing from the $u'v'$ term that is the most important; the forcing from the $u'u'$ term is more dominant further west and south where other factors not included in the model (e.g., associated with the separation of the baroclinic Gulf Stream jet from the continental slope) become important. These model calculations will be discussed in detail elsewhere.

We now turn to the Kuroshio extension region. We noted when discussing Fig. 7 that while there are clearly alternating bands of forcing from the zonally integrated zonal flow associated with the forcing arising from Reynolds stresses, these bands do not correspond to features in the zonally integrated zonal flow shown in the lower panel of the figure. There are several reasons for this. One is that the Kuroshio has a strong zonal component as it flows along the south coast of Japan prior to separation and this zonal component does contribute to the plot shown in the lower panel, obscuring the presence of the southern recirculation gyre that sits to the south of the Kuroshio extension. On the other hand, the northern recirculation, whose existence has only recently been established, is known not to have a surface signature but rather to be confined below about 1,000 m (Qiu et al. 2008 and Jayne et al. 2009) and so is not expected to appear in a plot of the zonally integrated surface zonal flow. Nevertheless, the bands of eastward and westward zonal momentum forcing implied by Fig. 7 do correspond to the latitude bands of the recirculation gyres as seen in observations. Furthermore, we believe that the Reynolds stresses computed at the surface, as in this paper and in Ducet and Le Traon (2001), act over the whole depth of the water column and should, therefore, be indicative for forcing at depth. We noted earlier that the strong dip in the blue curve in Fig. 7 near 32.5°N is related to the Kuroshio Large Meander. If we exclude this feature from the figure,

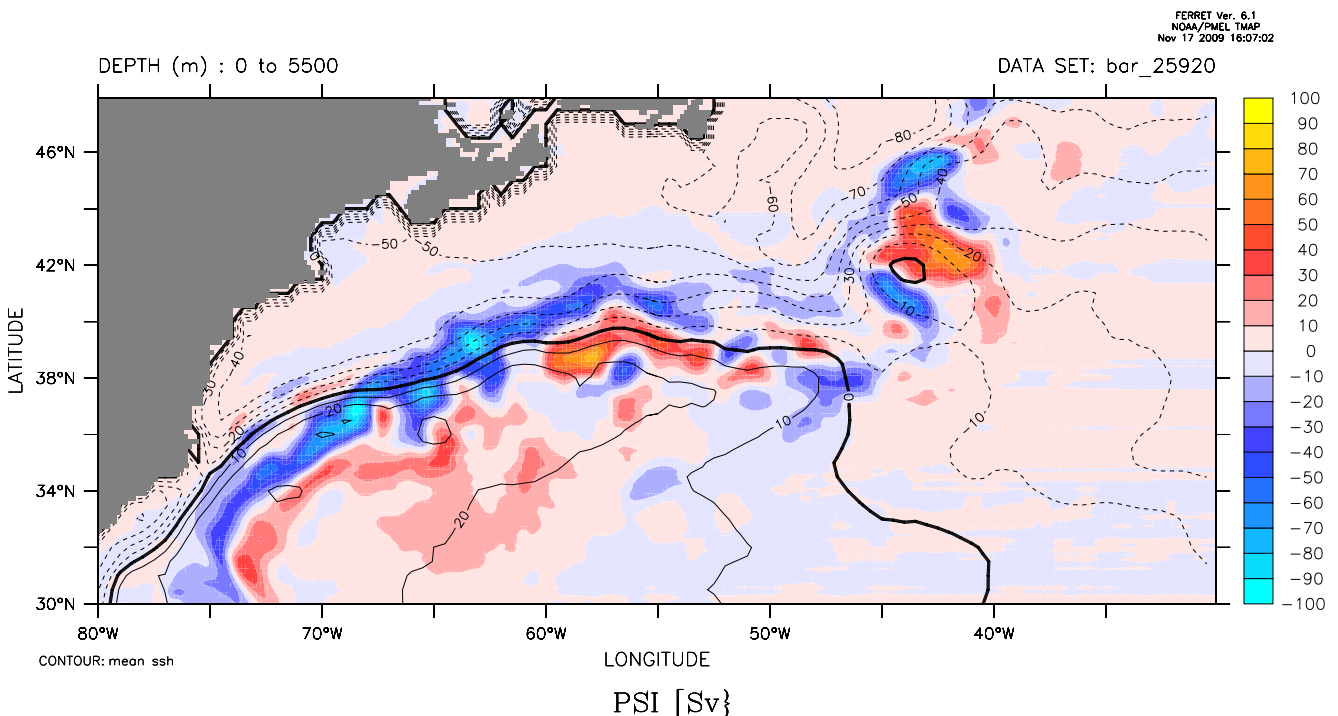
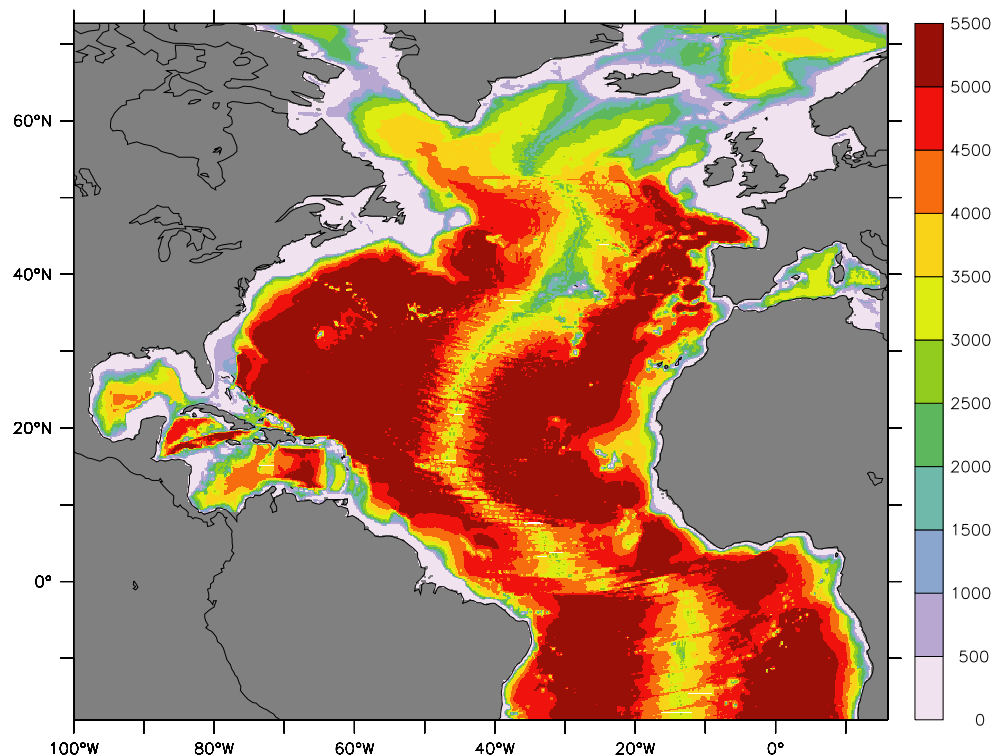


Fig. 8 The barotropic stream function (colour shading in units of Sverdrups) from a model with uniform density and realistic bottom topography and driven by the Reynolds stress forcings applied to the

zonal momentum equation. Also shown in the mean sea surface height taken from Niiler et al. (2003) with a contour interval of 0.1 m

Fig. 9 The model domain and bottom topography (colour shading in metres) used for the model calculation



there is then a region in which the gradient of the blue curve is positive, implying a westward momentum forcing of the zonally integrated flow in the same latitude band as the westward flow of the southern recirculation gyre. Likewise, the region of westward momentum forcing in the latitude band 35–36°N corresponds to the region of westward velocities in Fig. 4 of Qiu et al. (2008) based on float data and which they associate with the northern recirculation gyre. Qiu et al. (2008) have also shown that the Reynolds stress forcing for the zonal momentum equation (including the $u'u'$ term) from an eddying model acts to accelerate westward flow on the northern flank of the northern circulation gyre in the model. (This is the Earth Simulator hindcast run (Sasaki et al. 2008). It should be noted that in the model the recirculation gyre is shifted slightly to the north of the gyre seen in the observations). Qiu et al. (2008)'s result therefore confirms the impression from Fig. 7 that the Reynolds stress forcing is, indeed, important for the dynamics of the Kuroshio extension recirculation gyres.

5 Summary and discussion

We have updated the work of Ducet and Le Traon (2001) by using a longer time series (13 years compared to their 5 years) of satellite data to compute eddy momentum fluxes in the North Atlantic and North Pacific Oceans associated with the Gulf Stream and Kuroshio extensions. The spatial

pattern and magnitude of the eddy momentum fluxes is found to be remarkably similar when using the longer time series of data to that found in the early study, be it with some local differences in detail. It follows that the spatial pattern of the eddy momentum fluxes is robust, a feature we associate, following previous authors, with the influence of the underlying variable bottom topography (Hughes and Ash 2001; Ducet and Le Traon 2001). We noted that locally it is very difficult to see any evidence that eddies systematically feed momentum into the eastward jets of the Gulf Stream and Kuroshio extensions, a situation that stands in contrast to the situation in the atmosphere. The tendency for the variable bottom topography to scramble the eddy momentum fluxes in the ocean is consistent with the tendency of the variable bottom topography to distort the shape of the eddies. In the atmosphere, it is well-known that the shape of the eddies is very important for eddies to flux momentum (e.g. Hoskins et al. 1983; Marshall and Plumb 2008). The important role played by rough bottom topography is also revealed by the early, eddy-permitting numerical model experiment of Böning (1989) using an idealised box geometry. He found that including rough bottom topography inhibited the tendency of the model to produce zonal jets and the associated low frequency variability. Nevertheless, when considering the vertically and zonally integrated momentum budget for the zonally integrated zonal velocity, we find that the forcing from the eddy momentum flux becomes comparable in magnitude to the forcing from the zonal wind stress. We

have argued that for both the Gulf Stream and Kuroshio extensions that the momentum forcing from the Reynolds stresses does indeed play a role in driving the recirculation gyres in these two regions. Indeed, Qiu et al. (2008) have already shown, using output from an eddy model, that the Reynolds stress forcing for the zonal momentum equation is important for driving the northern recirculation gyre of the Kuroshio.

In recent years, many authors (Maximenko et al. 2005; Richards et al. 2006) have argued that zonal jets are a ubiquitous feature of the mid-latitude oceans and that these jets are driven by the eddy fluxes. However, for these zonal jets to be real, and not simply the result of time averaging the westward movement of an eddy (see Maximenko et al. 2005 where this possibility is discussed), there should be a systematic flux of momentum by the eddy momentum fluxes into these jets. Our results show that finding the required systematic eddy forcing of the jets may be difficult. Indeed, the important role played by the variable bottom topography in the ocean argues against their existence, although as in the numerical study of Böning (1989), such jets may be present in the thermocline. Clearly a careful study that attempts to relate the jets to the eddy momentum fluxes is required to resolve this issue.

Our work also has consequences for efforts to parameterise eddy momentum fluxes for use in non-eddy permitting ocean climate models, e.g. the ocean component of couple climate models. Given the importance of the variable bottom topography, parameterising the eddy momentum fluxes looks to be a daunting task. Ideally, some way of accounting for the distortion of the eddy shape by the variable bottom topography seems to be required. Given the difficulty of the problem, it may be that the current practice of parameterising the eddy flux of momentum using an eddy viscosity with a positive viscosity coefficient is the best one can do. On the other hand, our work also shows that the eddy flux of momentum is important in the momentum/vorticity budget, with systematic effects emerging after zonal and depth averaging. This raises concern that the current practice may not lead to sharp enough jets in parameterised models, and indeed to the lack of a representation of the recirculation gyres, as is indeed the case. There is evidence that for seasonal prediction purposes (e.g. Balmaseda et al. 2010), and also for climate modelling (e.g. Minobe et al. 2008), that accurate representation of the sea surface temperature is required suggesting that parameterised models need a better treatment of processes in the western boundary current extension regions. One option, at least in forecast models, may be the use of adjustment techniques such as that described by Greatbatch et al. (2004). Clearly, further research is required to resolve these issues.

Acknowledgements We are grateful to an anonymous reviewer whose comments proved helpful when revising the manuscript. This work has been funded by IFM-GEOMAR.

Appendix

The model is the MIT ocean general circulation model (see Marshall et al. (1997)). The model domain covers the North Atlantic basin from 100°W to 16°E and from 18°S to 72°N, uses realistic bottom topography (see Fig. 9) and is run with constant, uniform density. The horizontal resolution is one sixth degree in latitude and longitude. The model uses a height vertical coordinate and is run using partially filled cells at the bottom. There are 45 levels in the vertical with the spacing varying from 10 m near the surface to 250 m near the maximum depth of 5,500 m. The bottom topography is taken from the ETOPO5 data set. A biharmonic horizontal eddy viscosity is used with a value of $3 \times 10^{10} \text{ m}^4 \text{ s}^{-1}$, together with a vertical eddy viscosity with value $0.001 \text{ m}^2 \text{ s}^{-1}$. A linear bottom drag is implemented with coefficient $0.001 \text{ m}^2 \text{ s}^{-1}$. The only forcings used to drive the model are the Reynolds stresses derived from the satellite data and presented in this paper. It is assumed, for simplicity, that the Reynolds stresses vary linearly with depth from the surface to the bottom to reflect the equivalent barotropic vertical structure of eddies in the ocean (e.g. Wunsch (1997)). The model is run to steady state and it is the output in steady state that is shown in Fig. 8.

References

- Adamec D (1998) Modulation of the seasonal signal of the Kuroshio Extension during 1994 from satellite data. *J Geophys Res* 103:10209–10222
- Balmaseda MA, Ferranti F, Molteni F, Palmer T (2010) Impact of 2007 and 2008 Arctic sea ice anomalies on the atmospheric circulation: implications for long-range predictions. *Q J R Meteorol Soc* (submitted)
- Benedict JJ, Lee S, Feldstein SB (2004) Synoptic view of the North Atlantic oscillation. *J Atmos Sci* 61:121–144
- Böning CW (1989) Influences of a rough bottom topography on flow kinematics in an eddy-resolving circulation model. *J Phys Oceanogr* 19:77–97
- Clarke RA, Hill HW, Reiniger RF, Warren BA (1980) Current system south and east of the Grand Banks of Newfoundland. *J Phys Oceanogr* 10:25–65
- Ducet N, Le Traon P-Y (2001) A comparison of surface eddy kinetic energy and Reynolds stresses in the Gulf Stream and the Kuroshio Current systems from merged TOPEX/Poseidon and ERS-1/2 altimetric data. *J Geophys Res* 106:16603–16622
- Greatbatch RJ (1987) A model for the inertial recirculation of a gyre. *J Mar Res* 45:601–634
- Greatbatch RJ (2000) The North Atlantic oscillation. *Stoch Env Res Risk A* 14(4–5):213–242
- Greatbatch RJ, Sheng J, Eden C, Tang L, Zhai X, Zhao J (2004) The semi-prognostic method. *Cont Shelf Res* 24/18:2149–2165, Special issue on recent developments in physical oceanographic numerical modelling

- Haines K, Marshall JC (1987) Eddy-forced coherent structures as a prototype of atmospheric blocking. *Q J R Meteorol Soc* 113:681–704
- Hogg NG, Stommel H (1985) On the relation between the deep circulation and the Gulf Stream. *Deep-Sea Res* 32:1181–1193
- Hogg NG, Pickart RS, Hendry RM, Smethie WJ Jr (1986) The northern recirculation gyre of the Gulf Stream. *Deep-Sea Res* 33:1139–1165
- Holton JR (1981) An introduction to dynamic meteorology. Academic Press, Cleveland
- Hoskins BJ, James IN, White GH (1983) The shape, propagation and mean-flow interaction of large-scale weather systems. *J Atmos Sci* 40:1595–1612
- Hughes CW, Ash ER (2001) Eddy forcing of the mean flow in the Southern Ocean. *J Geophys Res* 106:2713–2722
- Jayne SR, Hogg NG, Waterman SN, Rainville L, Donohue KA, Watts DR, Tracey KL, McClean JL, Maltrud ME, Qiu B, Chen S, Hacker P (2009) The Kuroshio extension and its recirculation gyres. *Deep-Sea Res I* 56(12):2088–2099. doi:10.1016/j.dsr.2009.08.006
- Kawabe M (1985) Sea level variations at the Izu Islands and typical stable path of the Kuroshio. *J Oceanogr Soc Jpn* 41(5):307–326
- Kelly KA (1991) The meandering Gulf Stream as seen by the Geosat altimeter: surface transport, position, and velocity variance from 73°W to 46°W. *J Geophys Res* 96:16721–16738
- Kunz T, Fraedrich K, Lunkeit F (2009) Synoptic scale wave breaking and its potential to drive NAO-like circulation dipoles: a simplified GCM approach. *QJR Meteorol Soc* 135:1–19
- Le Traon P-Y, Nadal F, Ducet N (1998) An improved mapping method of multisatellite altimeter data. *J Atmos Oceanic Technol* 15:522–534
- Limpasuvan V, Hartmann D (1999) Eddies and the annular modes of climate variability. *J Geophys Res Lett* 26(20):3133–3136
- Mann CR (1967) The termination of the Gulf Stream and the beginning of the North Atlantic current. *Deep-Sea Res* 14:337–359
- Marshall JC, Plumb A (2008) Atmosphere, ocean and climate dynamics: an introductory text. Academic Press, Cleveland
- Marshall JC, Adcroft A, Hill C, Perelman L, Heisey C (1997) A finite-volume, incompressible Navier Stokes model for studies of the ocean on parallel computers. *J Geophys Res* 102:5753–5766
- Maximenko NA, Bang B, Sasaki H (2005) Observational evidence of alternating zonal jets in the world ocean. *Geophys Res Lett* 32: L12607. doi:10.1029/2005GL022728
- Minobe S, Kuwano-Yoshida A, Komori N, Xie S-P, Small RJ (2008) Influence of the Gulf Stream on the troposphere. *Nature* 452:206–209
- Morrow R, Church J, Coleman R, Chelton D, White N (1992) Eddy momentum flux and its contribution to the Southern Ocean momentum balance. *Nature* 357:482–484
- Niiler PP, Maximenko NA, McWilliams JC (2003) Dynamically balanced absolute sea level of the global ocean derived from near-surface velocity observations. *Geophys Res Lett* 30(22):2164. doi:10.1029/2003GL018628
- Nishida H, White WB (1982) Horizontal eddy fluxes of momentum and kinetic energy in the near-surface of the Kurishio Extension. *J Phys Oceanogr* 12:160–170
- Qiu B (1994) Determining the mean Gulf Stream and its recirculations through combining hydrographic and altimetric data. *J Geophys Res* 99:951–962
- Qiu B (1995) Variability of the Kuroshio Extension and its recirculation gyre from the first two-year TOPEX data. *J Phys Oceanogr* 25:1827–1842
- Qiu B, Chen S (2005) Variability of the Kuroshio Extension jet, recirculation gyre and mesoscale eddies on decadal time scales. *J Phys Oceanogr* 33:2465–2482
- Qiu B, Chen S (2009) Eddy-mean flow interaction in the decadal-modulating Kuroshio extension system. *Deep-Sea Res II*: (in press)
- Qiu B, Chen S, Hacker P, Hogg NG, Jayne SR, Sasaki H (2008) The Kuroshio Extension northern recirculation gyre: profiling float measurements and forcing mechanism. *J Phys Oceanogr* 38:1764–1779
- Richards KJ, Maximenko NA, Bryan FO, Sasaki H (2006) Zonal jets in the Pacific Ocean. *Geophys Res Lett* 33:L03605. doi:10.10129/2005GL024645
- Richardson PL (1985) Average velocity and transport of the Gulf Stream near 55°W. *J Mar Res* 43:83–111
- Sasaki H, Nonaka M, Masumoto Y, Sasai Y, Uehara H, Sakuma H (2008) An eddy-resolving hindcast simulation of the quasi-global ocean from 1950 to 2003 on the Earth Simulator. In: Ohfuchi W, Hamilton K (eds) High resolution numerical modelling of the atmosphere and ocean. New York, Springer
- Schmitz WJ (1980) Weakly depth-dependent segments of the North Atlantic circulation. *J Mar Res* 38:111–133
- Schmitz WJ (1982) A comparison of the mid-latitude eddy fields in the western North Atlantic and North Pacific oceans. *J Phys Oceanogr* 12:208–210
- Scott RB, Arbic BK, Holland CL, Sen A, Qiu B (2009) Zonal versus meridional velocity variance in satellite observations and realistic and idealized ocean circulation models. *Ocean Model* 23:102–112
- Shutts GJ (1983) The propagation of eddies in diffluent jet streams: Eddy vorticity forcing of “blocking” flow fields. *Q J R Meteorol Soc* 109:737–761
- Stammer D, Wunsch C (1999) Temporal changes in eddy energy of the oceans. *Deep-Sea Res II* 46:77–108
- Taft BA (1972) Characteristics of the flow of the Kuroshio south of Japan. In: Stommel H, Yoshida K (eds) Kuroshio—its physical aspects. Univ of Tokyo Press, Tokyo
- Tai CK, White WB (1990) Eddy variability in the Kuroshio Extension as revealed by Geosat altimetry: energy propagation away from the jet, Reynolds stresses, and seasonal cycle. *J Phys Oceanogr* 20:1461–1777
- Thompson R (1971) Why there is an intense eastward current in the North Atlantic but not in the South Atlantic. *J Phys Oceanogr* 1:235–237
- Thompson DWJ, Lee S, Baldwin MP (2002) Atmospheric processes governing the northern hemisphere annular Mode/North Atlantic Oscillation. In: Hurrell JW, Kushnir Y, Visbeck M, Ottersen G (eds) The North Atlantic Oscillation. AGU Monograph, Washington
- Vallis GK (2006) Atmospheric and oceanic fluid dynamics. Cambridge University Press, Cambridge
- Wardle R, Marshall JC (2000) Representation of eddies in primitive equation models by a PV flux. *J Phys Oceanogr* 30:2481–2503
- Webster F (1965) Measurement of eddy fluxes of momentum in the surface layer of the Gulf Stream. *Tellus* 18:239–245
- Worthington LV (1986) On the North Atlantic circulation. *Johns Hopkins Oceanogr Stud* 6. Johns Hopkins University, Baltimore
- Wunsch C (1997) The vertical partition of oceanic horizontal kinetic energy. *J Phys Oceanogr* 27:1770–1794
- Zhai X, Greatbatch RJ, Sheng J (2004) Diagnosing the role of eddies in driving the circulation of the northwest Atlantic Ocean. *Geophys Res Lett* 31:L23304. doi:10.1029/2004GL021146